Influence of Hydrodynamics on Liquid Mixing During Taylor Flow in a Microchannel

Yuanhai Su, Guangwen Chen, and Quan Yuan
Dalian National Laboratory for Clean Energy, Dalian Institute of Chemical Physics, Chinese Academy of Sciences, Dalian 116023, China

DOI 10.1002/aic.12698
Published online in Wiley Online Library (wileyonlinelibrary.com).

The miscible liquid-liquid two phases based on Taylor flow in microchannels was investigated by high-speed imaging techniques and Villermaux/Dushman reaction. The mixing based on Taylor flow was much better compared with that without introducing gas in microchannels, even the ideal micromixing performance could be obtained under optimized superficial gas and liquid velocities. In the mixing process based on Taylor flow, the superficial gas and liquid velocities affected the lengths and the velocities of Taylor bubble and liquid slug, and finally the micromixing performance. The formation process of Taylor flow in the inlets, the initial uniform distribution of reactants and the internal circulations in the liquid slug, and the thin liquid films all improved the mixing performance. Furthermore, a modified Peclet number that represented the relative importance of diffusion and convection in the mixing process was proposed for explaining and anticipating micromixing efficiency. © 2011 American Institute of Chemical Engineers AIChE J, 00: 000–000, 2011
Keywords: microchannel, Taylor flow, mixing, diffusion, multiphase flow, hydrodynamics

Introduction

Mixing processes of the miscible liquid-liquid two phases are well-known and widespread in chemical industry. Micromixing is mixing at the molecular scale, and is believed to play a very important role in the chemical process when the characteristics time scale of the chemical reaction involved is at the same magnitude or smaller than the time scale of the mixing process. Many reaction processes, such as precipitation and crystallization,[1,2] polymerization,[3] self-catalysis,[4] enzyme catalytic reaction,[5] etc., are determined by the micromixing efficiency. In these processes, the optimized micromixing performance can improve the contact of reactants at molecular scale, consequently, selectivity, yield, and quality of products. The development of new reactors for better micromixing efficiency is remarkable. From stirred tanks[6,7] to turbulent tube reactors,[8] static mixers with inner construction[9] and micromixers, the reactor design for better mixing performance has developed quickly.

During the last decade, microchemical engineering has experienced spectacular development as one of the most important process intensification technologies, which benefits from the miniaturization of channels and ducts within devices, where the characteristic lengths reach into the scale of boundary layers thickness.[10,11] Many microscale devices such as micromixers and microreactors have been designed elaborately, and attracted increasing attention in both laboratories and commercial areas in recent years.[12–18] Highly efficient mixing performance is a general character of these devices, and most of them are designed to realize rapid mixing.

The values of Reynolds number are usually low in microstructure devices, and flows in these devices are generally within the laminar flow regime. Therefore, the mixing is mainly driven by the molecular diffusion, and the diffusive time strongly depends on the diffusion length. A reduction of the diffusion distance, leads to enhanced macromixing, and eventually a significant improvement of micromixing. Moreover, increasing of the interfacial area of fluids and introducing advection were also proved to be another two effective methods for the improvement of the mixing in micromixers.[19] Based on these principles, a considerable variety of micromixers have been designed, such as interdigital micromixer,[20] split-and-recombine micromixer,[21] micromixer based on the collision of micro segments,[22] static micromixer,[23] multifunctional micromixer which made used of alternating current electroosmotic flow and asymmetric microelectrodes,[24] etc. However, these micromixers are difficult to manufacture due to the complexity of their structure, and their practical application usually was scarce. T-shaped and Y-shaped straight microchannels are easy to design and manufacture, so the hydrodynamics and the mixing performance in them are widely investigated. Soleymani et al.[25] carried out the numerical and experimental investigations of the liquid mixing in T-shaped microchannels. Their simulation results proved that the occurrence and the development of vortices in the T-junction of the microchannel were beneficial to the mixing performance, which both strongly depended on the flow rate, the aspect ratio and the throttle size of the microchannel, and the angle of two inlet channels. The mixing efficiency was not enough even the vortices in the T-junction improved the liquid mixing performance under large flow rates. Based on the results of the numerical simulations, they designed new micromixers with two junctions and circular elements in the mixing

Correspondence concerning this article should be addressed to G. Chen at gwchen@dicp.ac.cn.

channel, and the experiments showed that the mixing performance of these new micromixers was significantly better than that of the ordinary T-shaped microchannels. Sullivan et al.[26] used the lattice Boltzmann method to simulate the flow field and the subsequent analyte diffusion in a Y-shaped microchannel mixer, and compared the simulation results with the experimental data provided by magnetic resonance imaging. From their results, it was seen that the concentration distribution in the cross section of place closed to the microchannel exit was far away from the uniform condition; that is, the mixing efficiency in the Y-shaped microchannel was not enough. Although T-shaped and Y-shaped microchannel are usually used as research tools in laboratories, the mixing efficiency in both them is insufficient especially under low-flow rates.

Besides designing complex structures, introducing another immiscible phase to form multiphase flow including gas-liquid and liquid-liquid two-phase flows is also an efficient method to improve the liquid mixing performance in microchannels, which makes the mixing process limited in liquid slugs. Bringer et al.[27] had demonstrated that the mixing of multiple reagents could be isolated in slugs by introducing the immiscible organic phase to form multiphase flow in winding microchannels, and the chaotic advection appeared in slugs by internal circulations, which could stretch and fold the fluids striation, eventually the elimination of Taylor dispersion and the intensification of the mixing in slugs could be obtained. The potential application of the mixing based on liquid slugs exists in measure of fast reaction kinetics parameters,[28] protein crystallization,[29] synthesis of nanoparticles,[2] separation process,[30] improvement of selectivity for fast reaction, etc.[31]

The hydrodynamic characteristics play a very important role in the reactor design. Many investigators had characterized the gas-liquid two-phase flow patterns in microchannels.[32–34] Bubbly, slug, slug-annular, annular and churn flows are among the observed flow regimes in microchannels. Over a wide range of operating conditions, the flow in a microchannel is typically the so-called Taylor flow regime. Taylor flow is a special case of slug flow where bullet-shape gas bubbles (Taylor bubbles) are separated from each other by liquid slugs. The elongated bubble has a characteristic capsular shape with an equivalent diameter larger than the channel width, and the bubble itself is separated from the channel wall by a very thin liquid film. Salman et al.[35] had carried out the numerical study on the axial mixing in Taylor flow through circular microchannels. It was found that increasing film thickness resulted in larger and more distinct peaks in the unit cell residence-time distribution (RTD) curve, and the separation between the peaks increased while their size decreased with an increase in the length of the liquid slug. However, the experimental investigation about the mutual relationship between the hydrodynamics and the liquid mixing performance during Taylor flow has not been concerned up to now. Therefore, the strengthen mechanisms of the liquid mixing based on Taylor flow in microchannels should be systematically investigated for the operation optimization.

In this article, the main objective is to investigate the hydrodynamics of Taylor flow and the strengthen mechanisms of the liquid mixing based on Taylor flow in a microchannel. The macromixing (or mesomixing) was observed with high-speed imaging techniques, and the micromixing performance was studied by using the Villermaux/Dushman method. The liquid mixing process based on Taylor flow was compared with the mixing without introducing gas. The effects of the superficial gas and liquid velocities and the gas inlet locations on the hydrodynamics and the mixing performance were also studied. Moreover, a modified Peclet number for the liquid mixing based on Taylor flow was proposed, which could be used for explaining and anticipating the micromixing ratio (α).

Experimental Section

Villermaux/Dushman reaction

The micromixing performance of the mixers was evaluated by the Villermaux/Dushman method using a parallel competing reaction system.[36,37] This method has been used to study the degree of micromixing in a number of macro and micro mixers. The reactions involved in this method include the acid-catalyzed reaction of potassium iodide with potassium iodate to elemental iodine competing with the faster neutralization of the acid by a borate buffer-system:

$$H_2BO_3^- + H^+ \rightarrow H_3BO_3 \qquad (\text{quasi} - \text{instantaneous}) \tag{1}$$

$$5I^- + IO_3^- + 6H^+ \rightarrow 3I_2 + 3H_2O \qquad (\text{very fast}) \tag{2}$$

$$I_2 + I^- \leftrightarrow I_3^- \tag{3}$$

Reaction 1 is quasi-instantaneous, while (2) is fast but much slower than (1). However, Reaction 3 is an instantaneous equilibrium reaction. Under perfect micromixing conditions, the injected acid is instantaneously dispersed in the reactive medium and consumed by borates according to Reaction 1. Otherwise, the injected acid is consumed competitively by Reactions 1 and 2, and the formed I_2 can further react with I^- to yield triiodide complex (I_3^-) according to Reaction 3. The amount of I_3^- produced depends on the micromixing efficiency and can be easily measured by a spectrophotometer at 353 nm. The micromixing performance is less ideal, the more iodine is formed and the stronger light absorption (Abs) is detected. In our experiment there was a linear relationship between the light absorption and the concentration of I_3^-, which could be expressed as follows:

$$\text{Abs} = 22.54[I_3^-] \tag{4}$$

Based on the obtained concentration of I_3^-, the segregation index (X_S) that is defined to quantify the micromixing efficiency can be obtained:[38]

$$X_s = \frac{Y}{Y_{ST}} \tag{5}$$

$$Y = \frac{2(V_A + V_B)([I_2] + [I_3^-])}{V_B[H^+]_0} \tag{6}$$

$$Y_{ST} = \frac{6[IO_3^-]_0}{6[IO_3^-]_0 + [H_2BO_3^-]_0} \tag{7}$$

Y is the ratio of the acid mole number consumed by Reaction 2, to the total acid mole number injected, and Y_{ST} is the value of Y in the total segregation case when the

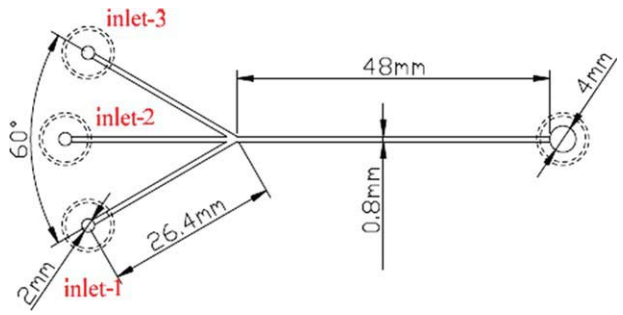

Figure 1. Schematic diagram of microchannel.

[Color figure can be viewed in the online issue, which is available at wileyonlinelibrary.com.]

micromixing process is infinitely slow. The value of X_S is within the range of $0 < X_S < 1$ for partial segregation and X_S equates to 0 for ideal mixing, while X_S equates to 1 for total segregation, respectively. In case of ideal mixing, the product distribution is solely governed by the kinetics of the reactions involved, and, thus, no iodine is found in the resulting mixtures. Based on the calculated X_S, the micromixing ratio (α) can be further obtained, which is defined by the ratio of the perfectly mixed volume to the totally segregated volume in the mixing process:

$$\alpha = \frac{1 - X_s}{X_s} \tag{8}$$

Experimental procedure

The microchannel was fabricated in the transparent PMMA substrate by the micromachining technology (FANUCKPC-30a) in our CNC Machining Center. The depth, the width, and the length of the main channel were 0.8 mm, 0.8 mm and 48 mm, respectively. Three inlet channels were connected to the main channel. The depth, the width, and the length of the inlet channels were 0.8 mm, 0.8 mm, 26.4 mm, and the two included angles between these inlet channels were both 30°. Another PMMA plate was used as a cover plate. The two plates were compressed each other by bolts. The schematic diagram of the main channel and the three inlet channels is shown in Figure 1.

The schematic diagram of experimental setup is shown in Figure 2. Aqueous solutions A and B were fed into the microchannel through two inlets by two high-precision piston pumps (Beijing Satellite Manufacturing Factory, measurement range: 0–5 mL/min, precision: ± 3%), and the volume flux ratio of solution A to solution B was fixed at 1. A solution was a mixture of potassium iodate (0.00234 mol/L), potassium iodide (0.0115 mol/L), sodium hydroxide (0.125 mol/L), and boric acid (0.25 mol/L). B solution was a dilute sulfuric acid solution, and its concentration was 0.0197 mol/L. Nitrogen was introduced into the microchannel from the inlet-2 or the inlet-3 by a mass flow controller (Beijing Sevenstar Electronics Co., measurement range: 0–50 mL/min, precision: ±1%), and directly emitted in the outlet of the microchannel. After collecting enough solution in a sample cell (ca. 3 mL), the light absorption of the effluent was measured within 30 s by a spectrophotometer (4802UV–VIS). Each experimental run was repeated at least three times, and each data point represented the mean value of at least three measurements of the light absorption, and the relative deviation did not exceed 5% in all the experiments. The flow patterns and the mixing process could be observed with a high-speed CCD camera that was connected to a personal computer. The solutions A and B were both replaced by deionized water, and a minute amount of methylene blue was dissolved in solution A for better visualization of the mixing phenomena. All experiments were conducted at room temperature (27-28°C).

Results and Discussion

Hydrodynamics and mixing in microchannels for single-phase flow without introducing gas

The transport processes such as mixing or heat transfer are greatly relevant to hydrodynamics in devices. The flow in microchannels is generally regarded as laminar flow because of low Reynolds numbers. Figure 3 shows the flow characteristics of the miscible liquid-liquid two phases in the microchannel without introducing gas. It is seen that there was a distinct diffusion boundary layer between the two miscible phases, especially for the extremely low Reynolds number ($Re_L = 25$). This diffusion boundary layer indicated that the mixing process was inefficient for these Reynolds numbers. For lower Reynolds number ($Re_L = 0.8$), Gunther and his coworkers[39] had reported that two streams containing 10-fold different concentrations of a fluorescent dye mixed by diffusion in the micochannel, the required mixing length was substantially longer than 1.0 m.

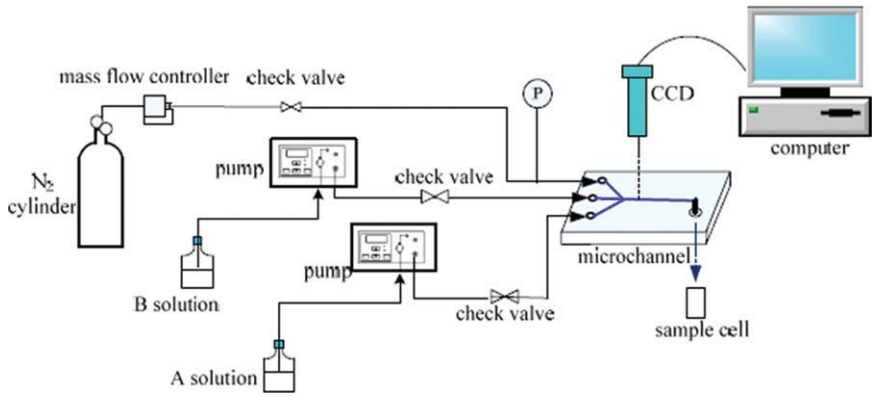

Figure 2. Schematic diagram of experimental setup.

[Color figure can be viewed in the online issue, which is available at wileyonlinelibrary.com.]

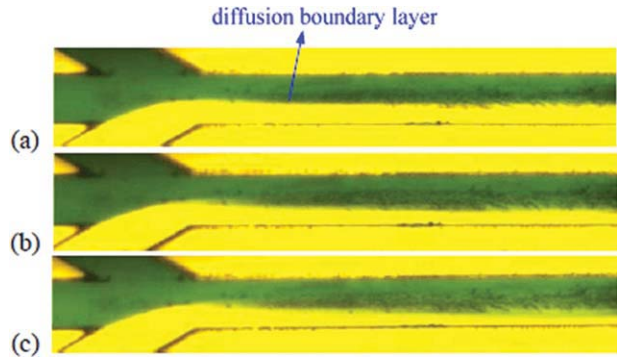

Figure 3. Flow characteristics of the miscible liquid-liquid two phases in the microchannel without introducing gas (a) j_L = 0.0313 m/s, Re_L = 25, (b) j_L = 0.104 m/s, Re_L = 83.3, and (c) j_L = 0.208 m/s, Re_L = 166.7.

[Color figure can be viewed in the online issue, which is available at wileyonlinelibrary.com.]

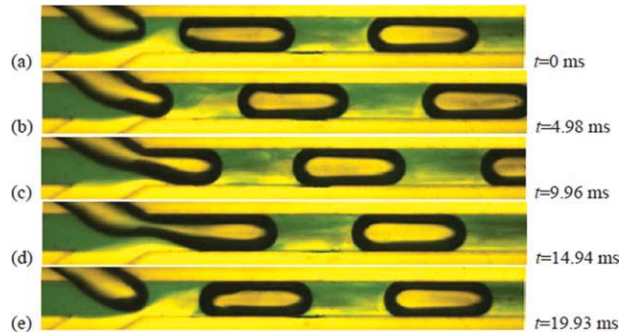

Figure 4. Typical pictures of Taylor bubble formation process in the squeezing regime in the microchannel (gas from inlet-3, j_L = 0.104 m/s, j_G = 0.118 m/s); (a) step 1, (b) step 2, (c) and (d) step 3, and (e) step 4.

[Color figure can be viewed in the online issue, which is available at wileyonlinelibrary.com.]

Hydrodynamics and liquid mixing process in the formation of Taylor flow

Garstecki et al.[40] thought the formation mechanism of Taylor flow in microchannels was mainly dependent on the relative magnitude of forces involved in this process, i.e., interfacial stress caused by surface tension, shear stress exerted on the tip of the gas by the liquid phase, resistance of flow to the liquid phase resulted from the partially blockage of the cross section of the main channel by the gas phase. Figure 4 shows a series of images taken during Taylor bubble formation in the microchannel, where the inlet-1 and the inlet-2 were used for the miscible liquid-liquid two phases, and the inlet-3 for the gas phase. The formations of Taylor bubble were all in the squeezing regime for our experiment, and the process was very typical (a) step 1, the gas-liquid two phases formed an interface at the inlets of the microchannel, and the gas continued to penetrate into the flowing liquids with a growing nearly hemispherical bubble tip, (b) step 2, the bubble was elongated and began to block almost the entire cross section of the microchannel when the diameter of the bubble tip approached the width of the microchannel, (c) and (d) step 3, the liquid pressure increased dramatically due to less available space for the flow of the liquid phases, which led to the squeezing of the gas neck, and (e) step 4, a Taylor bubble was produced after the rupture of the gas neck and a new cycle repeated again. The formation of Taylor bubble in the squeezing regime was also described in detail by other researchers.[34,41]

From this typical formation process of Taylor bubble, it was observed that the diffusion boundary layer between the miscible liquid-liquid two phases became more unclear. This phenomenon visually demonstrated that Taylor flow could dramatically intensify the liquid mixing in the microchannel. The space for the flowing of the miscible liquid-liquid two phases decreased quickly as the bubble grew up at the inlet, which led to much shorter diffusion distance between the miscible liquid-liquid two phases. The diffusion boundary layer was disturbed due to the increased liquid pressure at the inlets of the microchannel. These two aspects both effectively improved the liquid mixing in the microchannel inlets. After the rupture of the gas neck, the whole unit of Taylor bubble-liquid slug was formed. There were internal circulations in liquid slugs[27,42] due to the difference in the direction of motion of the fluid relative to the walls of the microchannel, hence, the radial mixing was improved, and the mixing process of the miscible liquid-liquid two phases was intensified. In addition, except for the formation of liquid slugs, a small part of the miscible liquid-liquid two phases was squeezed to the walls of the microchannel by Taylor bubbles, thus extremely thin liquid films were formed. The thin liquid films indicated that the diffusion distance was extremely short, and the large effective interfacial area (a), and the excellent mixing performance were obtained in these zones.

Effect of superficial gas velocity on hydrodynamics and liquid mixing process

The superficial gas velocity is one of most important operational parameters in Taylor flow in microchannels. Figure 5 shows the effect of the superficial gas velocity on Taylor flow and the liquid mixing in the microchannel at a fixed superficial liquid velocity. From these photographs, it is seen that the length of Taylor bubble increased with the

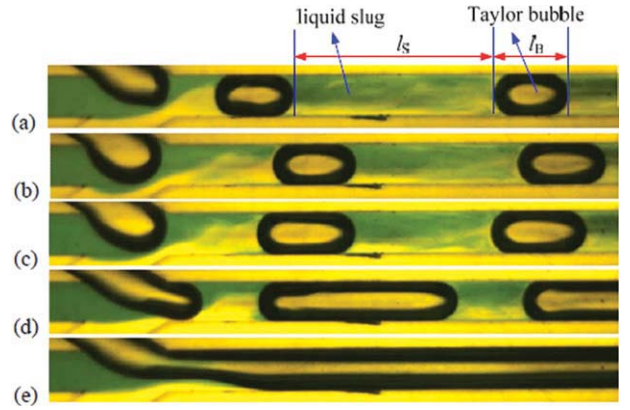

Figure 5. Effect of superficial gas velocity on hydrodynamics of Taylor flow in microchannels, j_L = 0.104 m/s, j_G (m/s); (a) 0.0148, (b) 0.0296, (c) 0.0592, (d) 0.237, and (e) 0.889.

[Color figure can be viewed in the online issue, which is available at wileyonlinelibrary.com.]

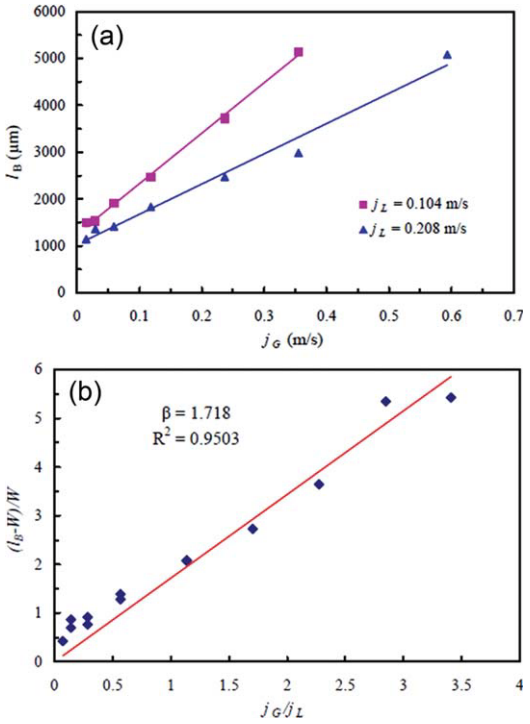

Figure 6. (a) Effects of the superficial gas and liquid velocities on the bubble length, and (b) Comparison between the measured Taylor bubble lengths and those predicted by the empirical correlation of Garstecki et al.

[Color figure can be viewed in the online issue, which is available at wileyonlinelibrary.com.]

increasing of the superficial gas velocity (Figure 5a–d), whereas the length of the liquid slug was just the opposite. As the superficial gas velocity was large enough, the gas occupied most of the space in the microchannel, and Taylor flow transformed into the slug-annular flow (Figure 5e).

For quantitative research, the lengths of Taylor bubbles and liquid slugs in the microchannel were measured from the corresponding images. Under each operational condition, a series of at least 10 images were analyzed and finally the average value was obtained (Figure 6a). As shown in Figure 6b, the lengths of Taylor bubbles in the squeezing regime could be approximately predicted by the simple scaling relation proposed by Garstecki et al.:[40]

$$\frac{l_B}{W} = 1 + \beta\frac{j_G}{j_L} \tag{9}$$

where β could be treated as a fitting parameter and its value depended on the inlet structure of the microchannel. Here, β was determined by the linear least square regression method, and its value was 1.718. According to the analysis of Garstecki et al.[40] β could be roughly treated as the ratio between the characteristic width of the neck when the gas phase fully entered the main microchannel and the width of the main microchannel. When nitrogen was introduced from the inlet-3, the inlet structure with three inlets could not be simplified as the inlet structure with two inlets, as shown in Figure 7. That is, the inlet structure with three inlets was not the equal of the T-shaped inlet structure used in the experiment of Garstecki et al.[40] In addition, the gas neck was thought to be a circular cross section and its diameter was comparable to the width of the main channel when the bubble began to span almost the entire cross section of the main channel (see Figure 4c). If these operations were carried out in T-shaped microchannels, the value of β in Eq. 9 should be close to 1. However, the fitting value (1.718) was larger than 1, and the reason may be as follows: the squeezing effect of the liquid phase was weaker as it was converged by two tributaries from the different inlets (inlet-1 and inlet-2).

The liquid slug length is an important hydrodynamic parameter which has been reported to have a very significant influence on the mass transfer process between the gas-liquid two phases in microchannels.[43] The liquid slug length of Taylor flow in microchannels is determined by the system parameters such as the superficial gas and liquid velocities, the fluid properties and the surface properties of the microchannel.[44,45] In general, increasing the gas velocity at a constant liquid velocity leads to shorter liquid slugs, and our experimental results demonstrated this principle, as shown in Figure 8a. Moreover, some researchers[46–48] had proposed empirical correlations for predicting the length of liquid slug of Taylor flow in microchannels due to its importance. In these correlations, the liquid slug length was correlated by considering Reynolds number, capillary number and gas holdup, and the Reynolds number was most emphasized. The following correlation based on the multiple linear regression analysis was found to predict the lengths of liquid slug well, which was similar to the correlation proposed by Liu et al.:[48]

$$\frac{l_s}{d_h} = 0.3694 Re_L^{0.585} Re_G^{-0.483} \tag{10}$$

Figure 8b demonstrates the experimental values of dimensionless liquid slug lengths vs. the predicted values by Eq. 10. It can be seen from Figure 8b that most of the relative deviations between the experimental and predicted values of dimensionless slug lengths were within ±20%. From these

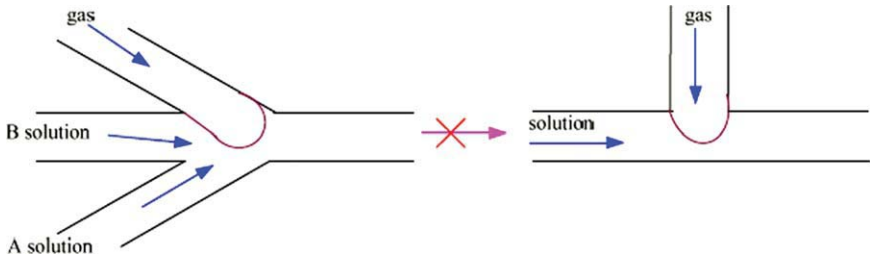

Figure 7. Schematic diagram of different inlet structures (gas from inlet-3).

[Color figure can be viewed in the online issue, which is available at wileyonlinelibrary.com.]

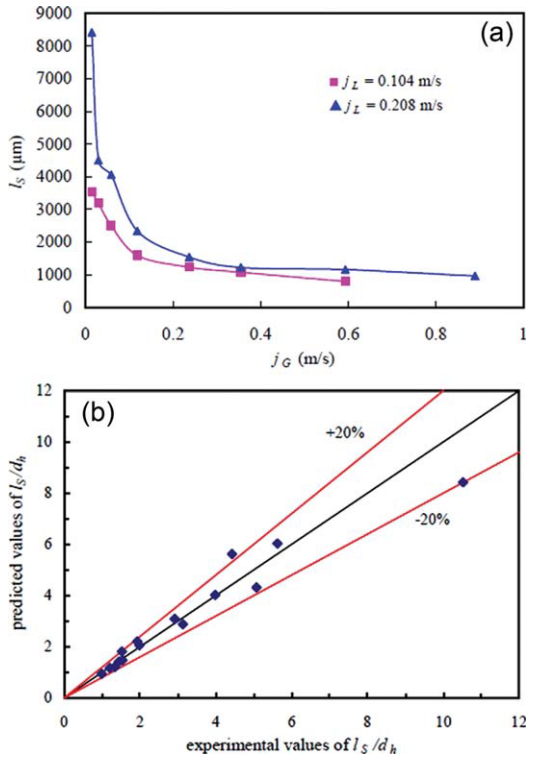

Figure 8. (a) Effects of the superficial gas and liquid velocities on liquid slug length, and (b) comparison between experimental values of dimensionless liquid slug lengths vs. the predicted values.

[Color figure can be viewed in the online issue, which is available at wileyonlinelibrary.com.]

correlations 9 and 10 it is validated that the superficial gas and liquid velocities are both controllable parameters, which affect the hydrodynamics of Taylor flow when the fluid system and microchannel have been determined.

From Figure 5 it can also be seen that the concentration of methylene blue in the liquid slug tended to be homogeneous with the increasing of the superficial gas velocity, which demonstrated the liquid mixing process was strengthened. As the superficial gas velocity increased, shorter liquid slug was obtained. Therefore, the intensity of the internal circulations in the liquid slug became more drastic, the radial mixing and finally the liquid mixing process were improved. In other cases, as the superficial gas velocity was large enough (Figure 5e), the slug-annular flow or the annular flow was predominate in the gas-liquid two-phase patterns in our experiment. At that time, most part of the miscible liquid-liquid two phases was squeezed to the walls of the microchannel and formed extremely thin liquid films. The diffusion distance was reduced and the effective interfacial area was increased dramatically, and the whole mixing process was excellent.

Effect of gas inlet locations on hydrodynamics and liquid mixing process

Zheng et al.[49] had experimentally demonstrated that the mixing rate in the liquid slug with alternant distribution of reactants was faster than that with parallel distribution for the immiscible liquid-liquid two-phase system in microchannels. In order to investigate the effect of the gas inlet locations on the hydrodynamics and the liquid mixing process in Taylor flow, nitrogen was introduced into the microchannel from the inlet-2. As shown in Figure 9, the formation of Taylor bubble was also in the squeezing regime. However, the formation process of Taylor bubble when the gas was introduced from the inlet-2 was a little different from that when the gas from the inlet-3. The formation process was comparatively free when the gas was introduced from the inlet-2, and the miscible liquid-liquid two phases from the inlet-1 and the inlet-3, that is, the confined room became larger and the total force from the miscible liquid-liquid two phases was weakened. Therefore, the formation frequency of the unit of Taylor bubble and liquid slug decreased, and the lengths of Taylor bubbles (Figure 10a) and the liquid slugs (Figure 10b) became larger at the same superficial gas and liquid velocities.

In addition, it is seen from Figure 9 that the formation of Taylor bubble was axisymmetrical when the gas was introduced from the inlet-2, and there was an obvious diffusion boundary layer between the miscible liquid-liquid two phases in the initial liquid slug. The diffusion boundary layer indicated that the initial distribution of substances in the liquid slug was far from the homogeneous condition. Although the diffusion boundary layer also became more and more indistinct as the liquid slug flowed through the microchannel, the intensity was not evident enough, which illustrated the relatively weaker effect of the internal circulations on the radial mixing. These phenomena indicated the liquid mixing process based on Taylor flow when the gas was introduced from inlet-2 was not as efficient as the gas from inlet-3.

Micromixing in microchannels for single-phase flow without introducing gas

The hydrodynamics in microchannels can be photographed by the high-speed CCD camera, thus, the mixing process of the miscible liquid-liquid two phases can be visually observed. However, these high-speed imaging techniques can only provide information in macroscale or mesoscale. In the following sections, the micromixing performance in microchannels with and without introducing gas was investigated by using the "Villermaux/Dushman" method.

As discussed previously, the flow of the miscible liquid-liquid two phases in the microchannel without introducing gas was laminar flow because of low Reynolds numbers. Also, there was a distinct diffusion boundary layer between the two miscible phases. The inefficient macromixing (or

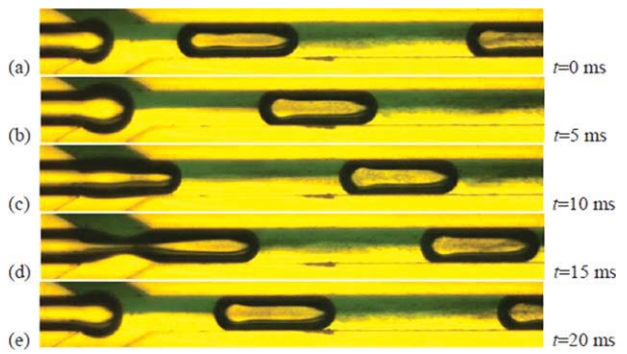

Figure 9. Typical pictures of Taylor bubble formation process in the squeezing regime in the microchannel (gas from inlet-2, j_L = 0.208 m/s, j_G = 0.118 m/s).

[Color figure can be viewed in the online issue, which is available at wileyonlinelibrary.com.]

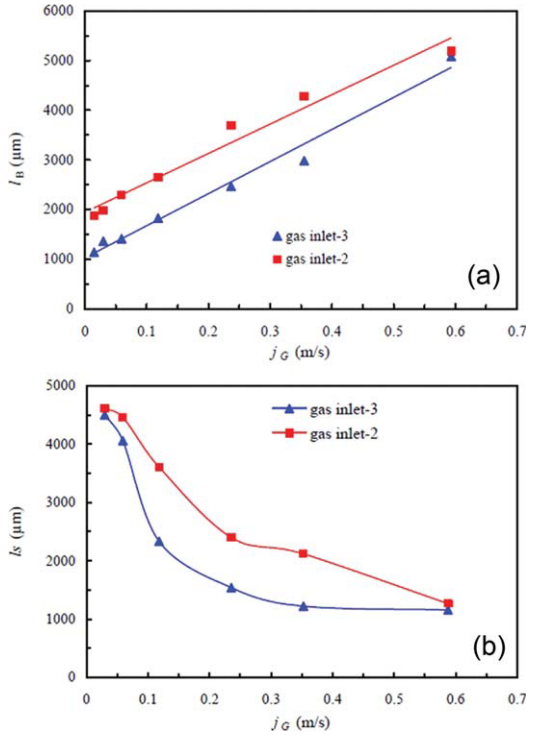

Figure 10. Effect of the gas inlet positions on the lengths of Taylor bubbles (a), and liquid slugs (b), j_L = 0.208 m/s.

[Color figure can be viewed in the online issue, which is available at wileyonlinelibrary.com.]

mesomixing) must result in low-micromixing efficiency. As shown in Figure 11, the light absorption decreased with an increase in Re_L due to the weak interface disturbance, however, the minimum value of the light absorption still reached 0.725. These large values of the light absorption indicated that the micromixing performance in the microchannel for single-phase flow was far from the ideal micromixing condition.

Effect of superficial gas velocity on micromixing performance

Figure 12 shows the effect of superficial gas velocity on the micromixing performance in the microchannel for two different superficial liquid velocities. It is seen that the values of the light absorptions were large without introducing gas, and quickly decreased with the increasing of superficial gas velocity, and finally tended to extremely low values. For the superficial liquid velocity (j_L = 0.104 m/s), and the superficial gas velocity (j_G = 1.325 m/s), the light absorption was as low as 0.0013, which was close to the range of apparatus detection error (0.001). The extremely low light absorptions demonstrated that the micromixing performance based on Taylor flow was much better compared to that based on the single-phase flow without introducing gas, even the ideal micromixing performance could be obtained under optimized superficial gas and liquid velocities. The parallel flow of the miscible liquid-liquid two phases could be easily transformed to Taylor flow by introducing the gas in microchannels. As the superficial gas velocity increased, the length of the liquid slug was decreased and its velocity was increased ($U_S = j_L + j_G$). Therefore, the internal circulations

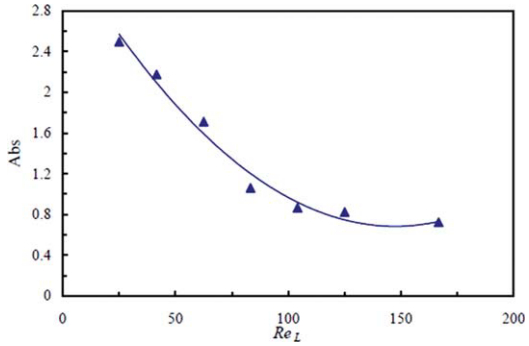

Figure 11. Effect of Re_L on micromixing performance in microchannel (without introducing gas).

[Color figure can be viewed in the online issue, which is available at wileyonlinelibrary.com.]

in liquid slugs were enhanced, which were beneficial to the radial mixing and the micromixing process.

Moreover, the zones of thin liquid films provided extremely short diffusion distance and large effective interfacial area for the mixing process. The thickness of the liquid film around a Taylor bubble in rectangular microchannels is nonuniform, which varies in both lateral and axial directions from the bubble nose to its tail. It is difficult to determine the liquid film thickness from the 2-D optical images of Taylor flow in our experiment. In a review Kreutzer et al.[50] pointed out that the following correlation proposed by Aussillous and Quéré[51] could predict well the thickness of the liquid film for round microchannels:

$$\frac{\delta}{d} = \frac{0.66Ca^{2/3}}{1 + 3.33Ca^{2/3}} \tag{11}$$

where δ, d and Ca were thickness of liquid film, diameter of microchannel and capillary number ($\mu U_S/\gamma$), respectively. Here, we use this correlation to approximately calculate the thickness of the liquid film around a Taylor bubble in the rectangular microchannel. The value of Ca was in the range of 1.41×10^{-3}–1.83×10^{-2} as the superficial gas velocity increased, so the thickness of the liquid film was in the range of 6.38–29.77 μm. It is well known that the mixing time depends on the diffusion distance. Consequently, as the diffusion distance was reduced from several hundreds

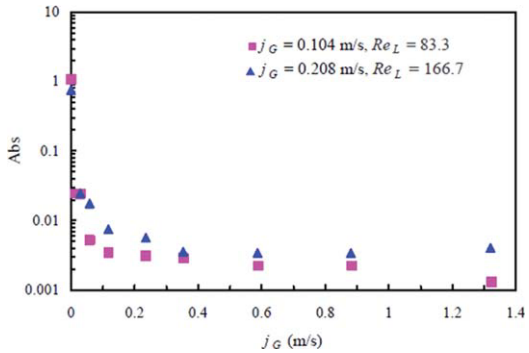

Figure 12. Effect of superficial gas velocity on micromixing performance (gas from inlet-3).

[Color figure can be viewed in the online issue, which is available at wileyonlinelibrary.com.]

micrometers to several tens micrometers even to several micrometers, the mixing time was significantly shortened, and the micromixing performance in these thin liquid film zones was improved obviously. Some researchers also had demonstrated that the mass transfer and reaction process were further improved in these thin liquid films between Taylor bubble and microchannel wall.[52,53]

From Figure 12 it is also seen that the light absorptions for the lower superficial liquid velocity were somewhat lower compared to those for the higher liquid velocity at the same superficial gas velocity, that is, the micromixing performance was better for lower superficial liquid velocity. This may be attributed to the different hydrodynamics in the microchannel. As shown in Figure 8a, the length of the liquid slug in Taylor flow was shorter for the lower superficial liquid velocity at the same superficial gas velocity; accordingly the internal circulations in the shorter liquid slug were more intense.

Effect of gas inlet locations on micromixing performance

As mentioned before, the gas inlet locations had great effects on the formation frequencies of Taylor bubble and the liquid slug and their lengths, and the initial concentration distribution of reactants in liquid slugs in the microchannel. Therefore, the micromixing performance based on Taylor flow must be influenced by the gas inlet locations. Figure 13 shows the effect of the gas inlet locations on the micromixing performance under different superficial gas and liquid velocities. As expected, the micromixing performance when the gas was introduced from the inlet-3 of the microchannel was superior compared with that when the gas from inlet-2, especially at low superficial gas velocities. It is well known that there are two symmetrical internal circulations in the liquid slug of Taylor flow in the straight microchannel, and the two internal circulations are beneficial to the radial mixing in the liquid slug.[27] As the gas was introduced from the inlet-3, the formation of the unit of Taylor bubble-liquid slug was asymmetrical. Under the circumstances, the initial distribution of reactants in the liquid slug was comparatively uniform, which could be observed in the formation process of Taylor flow. Moreover, the strength of internal circulations is relevant to the length of the liquid slug, and the shorter liquid slug leads to more effective internal circulations. As the miscible liquid-liquid two phases were introduced from inlet-1 and inlet-2 and the gas from inlet-3, the squeezing action of the liquid phases on the gas was more effective, thus shorter Taylor bubbles and liquid slugs were obtained. Therefore, better micromixing performance could be obtained when the gas was introduced from inlet-3.

As the superficial gas velocity was enough, the effect of the gas inlet locations on the micromixing performance was relatively weak. This situation was more obvious at the low-superficial liquid velocity (Figure 13b). At that time, the gas-liquid two-phase pattern tended to form the slug-annular flow whenever the gas was introduced from inlet-2 or inlet-3, and most of the miscible liquid-liquid two phases was squeezed to the walls of the microchannel to form thin liquid films. Therefore, the extremely short diffusion distance and the large effective interfacial area and almost the ideal micromixing performance were obtained for the two different gas inlet locations.

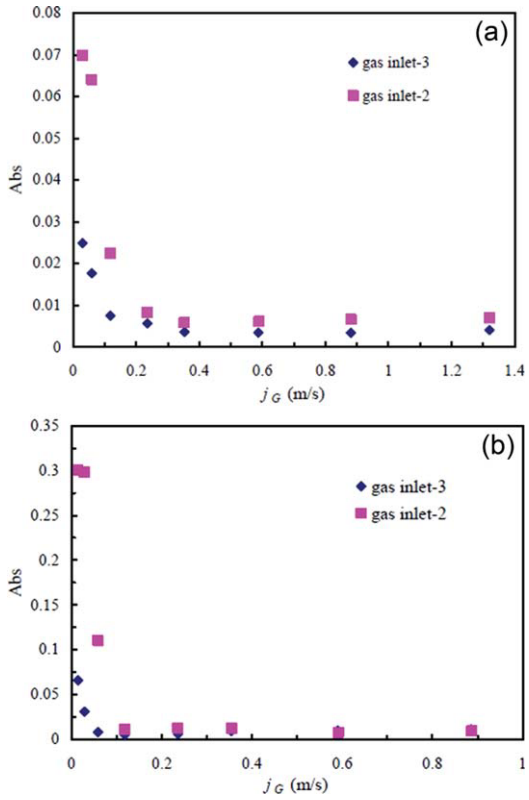

Figure 13. Effect of the gas inlet locations on micromixing performance (a) j_L = 0.208 m/s, Re_L = 166.7, (b) j_L = 0.0313 m/s, Re_L = 25.

[Color figure can be viewed in the online issue, which is available at wileyonlinelibrary.com.]

Modified Peclet number for micromixedness ratio

As discussed in the earlier sections, the micromixing performance in microchannels was intensified dramatically by the Taylor flow approach. The micromixing efficiency in the liquid slug was dependent on the length and the velocity of the liquid slug, and the initial distribution of reactants. These experimental results were similar to the numerical simulation results of Tanthapanichakoon et al.[54] They reported the mixing characteristics inside a microfluidic liquid slug of immiscible liquid-liquid two phases using the computational fluid dynamics (CFD) simulations. Their simulation results provided insights into the influences of operating parameters on the rate of slug-based mixing (such as initial arrangement of reactants in liquid slugs, slug velocity and slug diameter), and Peclet number of liquid slugs ($Pe = U_S d_{Diff}^2 / l_S D$) for estimating mixing rates and designing liquid slugs was proposed based on the simulation results. However, it deserves to be noted that the situation of introducing gas to form multiphase flow is different from that of introducing organic phase, in which the gas phase is dispersed phase and the aqueous phase is continuous. That is, the liquid slugs are connected with each other by the liquid films, and the mixing process of the miscible liquids occurs both in liquid slugs and the liquid films for the gas-liquid two-phase system in the microchannel. Furthermore, the separation of the gas-liquid two phases after the outlet of microchannel is much easier than that of the immiscible liquid-liquid two phases because of larger density difference between the gas-liquid two phases.

Actually, the Peclet number proposed by Tanthapanichakoon et al.[54] was the ratio of the diffusive time scale ($t_{Diff} = d_{Diff}^2/D$), to the convective transport time scale ($t_{Conv} = l_S/U_S$) in liquid slugs, where d_{Diff} was the diffusion distance and considered to be equal to the hydraulic diameter of the microchannel. When the Peclet number was less than a constant value, the mixing in liquid slugs was controlled by the molecular diffusion, or else, it was determined by the convective transport. The internal circulations can be considered as a way of convective transport, which quicken the distributions of reactants in liquid slugs. Here, we investigate the relationship between Peclet number and the micromixing efficiency in liquid slugs for gas-liquid two-phase systems, and use the micromixing ratio to represent the micromixing efficiency. Although the flow in liquid film zones of Taylor flow in microchannels is considered as laminar flow, the micromixing performance is excellent due to extremely short diffusion distance and large effective interfacial area. Therefore, the diffusive time scale is determined by two zones, one is the liquid slug zone, and the other is the liquid film zone. The diffusive timescale is reduced due to the liquid film zone, that is, it can be expressed as the function of liquid film ($f(\delta, l_F)$):

$$t_{Diff} = \frac{d_{Diff}^2}{D} \cdot \frac{1}{1 + f(\delta,\ l_F)} \tag{12}$$

where δ and l_F are the thickness and the length of the liquid film, respectively. As discussed previously, the thickness of liquid films was less than 30 μm in the operating range of superficial gas and liquid velocities, so the mixing could be considered to be finished instantaneously in the liquid film zone, and the contribution of the liquid film was determined by its length. The function of liquid film can be further expressed as the following equation:

$$f(\delta,\ l_F) = f(l_F) \tag{13}$$

For dimensionless treatment, $f(\delta,\ l_F)$ is expressed as the following:

$$f(l_F) = \frac{l_F}{l_F + l_S} = \frac{l_B}{l_B + l_S} \tag{14}$$

where the length of the liquid film (l_F) is considered to be approximately equal to the length of Taylor bubble (l_B). The physical meaning of $f(l_F)$ is the ratio of the length of Taylor bubble to the length of the whole unit of Taylor bubble-liquid slug. Based on aforementioned analysis, a modified Peclet number (Pe^*) in microchannels for gas-liquid two-phase systems is proposed, as given in the following:

$$Pe^* = \frac{U_S d_{\mathrm{Diff}}^2}{l_S D} \cdot \frac{1}{1 + \frac{l_B}{l_B + l_S}} = \frac{l_B + l_S}{2l_B + l_S} \cdot \frac{U_S d_{\mathrm{Diff}}^2}{l_S D} \tag{15}$$

As the mixing of the miscible liquid-liquid two phases is carried out in microchannels without introducing gas, l_B, l_S, U_S are considered to be equal to 0, the length of the microchannel (l), and the mean velocity of the miscible liquid-liquid two phases (U_M or j_L), respectively. At that time, the modified Peclet number (Pe^*) can be further simplified as the following equation:

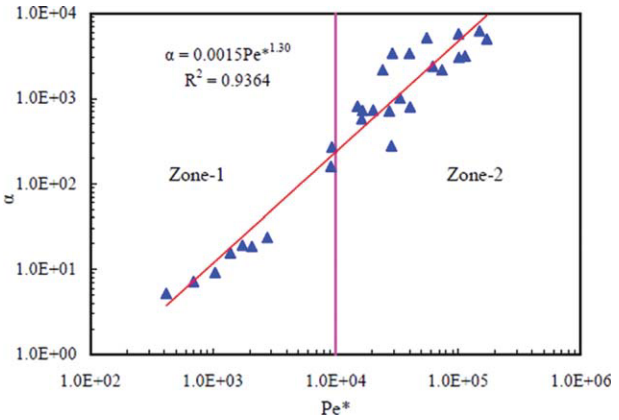

Figure 14. Effect of *Pe on micromixing ratio in microchannels.**

[Color figure can be viewed in the online issue, which is available at wileyonlinelibrary.com.]

$$Pe^* = \frac{U_M d_{\mathrm{Diff}}^2}{lD} \tag{16}$$

Figure 14 shows the relationship between Pe^* and the micromixedness ratio, where D was set at 10^{-9} m^2/s. It is seen that α increased with the increasing of Pe^*, and they approximately satisfied the power function:

$$\alpha = 0.0015(Pe^*)^{1.30} \tag{17}$$

The results demonstrated that Pe^* is an important parameter in microchannels for the liquid mixing processes, it must increase Pe^* to obtain higher micromixng efficiency. In Figure 14, the whole zone was divided Zone-1 ($Pe^* < 10^4$) and Zone-2 ($Pe^* > 10^4$). In Zone-1, the micromixing efficiency was determined by the diffusion, and all operations without introducing gas into the microchannel were in this zone. Most of operations based on Taylor flow were in Zone-2, where the micromixing efficiency was mainly controlled by the convection caused by internal circulations in liquid slugs.

Conclusion

The mixing of the miscible liquid-liquid two phases based on Taylor flow in microchannels was investigated by high-speed imaging techniques and the Villermaux/Dushman reaction system. It was found that the mixing and the micromixing performances based on Taylor flow were much better compared with those without introducing gas. The formation model of Taylor flow was in the squeezing regime in our experiment. The restricted flow of the liquid phases, the internal circulations in the liquid slug, and the thin liquid film all improved the liquid mixing in the formation process of Taylor flow. The lengths of Taylor bubbles and liquid slugs depended on the superficial gas and liquid velocities, which could be predicted by empirical correlations. Higher superficial gas velocity led to shorter liquid slug and longer Taylor bubble, which was beneficial to the mixing and the micromixing performances in the microchannel. The ideal micromixing performance could be obtained under optimized superficial gas and liquid velocities in the microchannel. In addition, the gas inlet location affected the lengths of Taylor bubble and the liquid slug, the initial distribution of reactants

in the liquid slug, and finally the micromixing performance. Based on experimental results, a modified Peclet number that represented the relative importance of diffusion and convection in the mixing process was proposed for explaining and anticipating micromixing ratio. It must increase the value of Pe^* to obtain higher micromixing efficiency in microchannels for the liquid mixing.

Acknowledgments

The work reported in this article was financially supported by research grants from the National Natural Science Foundation of China (Nos. 20906087, 20911130358), Ministry of Science and Technology of China (No. 2009CB219903) and Fund of Dalian Institute of Chemical Physics, CAS (No. K2009D01).

Notation

Abs = light absorption, 1
a = effective interfacial area, m^2/m^3
C_a = capillary number, 1
C_j = concentration of species j, $mol \cdot L^1$
C_{j0} = environmental concentration of species j, $mol \cdot L^1$
d = diameter of microchannel, m
d_h = hydraulic diameter of microchannel, m
d_{Diff} = diffusion distance, m
D = diffusivity, m^2/s
j_L = superficial liquid velocity, m/s
J_G = superficial gas velocity, m/s
l = length of microchannel, m
l_B = length of Taylor bubble, m
l_F = length of liquid film, m
l_S = length of liquid slug, m
Pe = Peclet number, 1
Pe^* = modified Peclet number, 1
Re = Reynolds number, 1
Re_L = liquid-phase Reynolds number, 1
Re_G = gas-phase Reynolds number, 1
t_{Diff} = diffusive time scale, s
t_{Conv} = convective transport time scale, s
U_S = liquid slug velocity, m/s
V_A = volumetric flow rate of A solution, mL/min
V_B = volumetric flow rate of B solution, mL/min
W = width of microchannel
X_s = segregation index, 1
Y = ratio of acid mole number consumed by Reaction 2 to the total acid mole number injected, 1
Y_{ST} = value of Y in the total segregation case, 1

Greek letters

δ = thickness of liquid film, m
α = micromixedness ratio, 1
β = fitting constant in Eq. 9
μ = liquid phase viscosity, Pa·s
γ = surface tension, N/m

Subscripts

B = Taylor bubble
F = liquid film
L = liquid phase
G = gas phase
S = liquid slug

Literature Cited

1. Baldyga J, Orciuch W. Barium sulphate precipitation in a pipe - an experimental study and CFD modelling. *Chem Eng Sci*. 2001;56:2435–2444.
2. Khan SA, Jensen KF. Microfluidic synthesis of titania shells on colloidal silica. *Adv Mater*. 2007;19:2556–2560.
3. Engelmann U, Schmidtnaake G. Influence of micromixing on the free-radical polymerization in a discontinuous process. *Macromol Theor Simul*. 1994;3:855–883.
4. Bourne JR. Mixing on the molecular scale (Micromixing). *Chem Eng Sci*. 1983;38:5–8.
5. Giridhar M, Krishnaiah K. The effect of micromixing and macromixing on enzyme reaction in a real Cstr. *Bioprocess Eng*. 1993;9:263–269.
6. Yao WG, Sato H, Takahashi K, Koyama K. Mixing performance experiments in impeller stirred tanks subjected to unsteady rotational speeds. *Chem Eng Sci*. 1998;53:3031–3040.
7. Assirelli M, Bujalski W, Eaglesham A, Nienow AW. Study of micromixing in a stirred tank using a Rushton turbine - Comparison of feed positions and other mixing devices. *Chem Eng Res Des*. 2002;80:855–863.
8. Barresi AA, Marchisio D, Baldi G. On the role of micro- and mesomixing in a continuous Couette-type precipitator. *Chem Eng Sci*. 1999;54:2339–2349.
9. Liu SP, Hrymak AN, Wood PE. Laminar mixing of shear thinning fluids in a SMX static mixer. *Chem Eng Sci*. 2006;61:1753–1759.
10. Kochmann N. *Transport Phenomena in Micro Process Engineering*. New York: Springer; 2007.
11. Gerven TV, Stankiewicz A. Structure, energy, synergy, times-the fundamentals of process intensification. *Ind Eng Chem Res*. 2009;48:2465–2474.
12. Ehrfeld W, Golbig K, Hessel V, Löwe H, Richter T. Characterization of mixing in micromixers by a test reaction: Single mixing units and mixer arrays. *Ind Eng Chem Res*. 1999;38:1075–1082.
13. Hessel V, Löwe H. Microchemical engineering: Components, plant concepts user acceptance - Part I. *Chem Eng Technol*. 2003;26:13–24.
14. Ying Y, Chen GW, Zhao YC, Li SL, Yuan Q. A high throughput methodology for continuous preparation of monodispersed nanocrystals in microfluidic reactors. *Chem Eng J*. 2008;135:209–215.
15. Zhang HC, Chen GW, Yue J, Yuan Q. Hydrodynamics and mass transfer of gas-liquid flow in a falling film microreactor. *AIChE J*. 2009;55:1110–1120.
16. Wiles C, Watts P. Continuous flow reactors, a tool for the modern synthetic chemist. *Eur J Org Chem*. 2008;1655–1671.
17. Wong SH, Ward MCL, Wharton CW. Micro T-mixer as a rapid mixing micromixer. *Sensor Actuat B-Chem*. 2004;100:359–379.
18. Men Y, Hessel V, Löb P, Löwe H, Werner B, Baier T. Determination of the segregation index to sense the mixing quality of pilot- and production-scale microstructured mixers. *Chem Eng Res Des*. 2007;85:605–611.
19. Hessel V, Löwe H, Schönfeld F. Micromixers - a review on passive and active mixing principles. *Chem Eng Sci*. 2005;60:2479–2501.
20. Ehrfeld W, Golbig K, Hessel V, Löwe H, Richter T. Characterization of mixing in micromixers by a test reaction: Single mixing units and mixer arrays. *Ind Eng Chem Res*. 1999;38:1075–1082.
21. Schönfeld F, Hessel V, Hofmann C. An optimised split-and-recombine micro-mixer with uniform 'chaotic' mixing. *Lab Chip*. 2004;4:65–69.
22. Nagasawa H, Aoki N, Mae K. Design of a new micromixer for instant mixing based on the collision of micro segments. *Chem Eng Technol*. 2005;28:324–330.
23. Bertsch A, Heimgartner S, Cousseau P, Renaud P. Static micromixers based on large-scale industrial mixer geometry. *Lab Chip*. 2001;1:56–60.
24. Kim BJ, Yoon SY, Lee KH, Sung HJ. Development of a microfluidic device for simultaneous mixing and pumping. *Exp Fluids*. 2009;46:85–95.
25. Soleymani A, Kolehmainen E, Turunen I. Numerical and experimental investigations of liquid mixing in T-type micromixers. *Chem Eng J*. 2008;135:S219–S228.
26. Sullivan SP, Akpa BS, Matthews SM, Fisher AC, Gladden LF, Johns ML. Simulation of miscible diffusive mixing in microchannels. *Sens Actuators B-Chem*. 2007;123:1142–1152.
27. Bringer MR, Gerdts CJ, Song H, Tice JD, Ismagilov RF. Microfluidic systems for chemical kinetics that rely on chaotic mixing in droplets. *Philos Trans R Soc A*. 2004;362:1087–1104.
28. Song H, Ismagilov RF. Millisecond kinetics on a microfluidic chip using nanoliters of reagents. *J Am Chem Soc*. 2003;125:14613–14619.
29. Zheng B, Tice JD, Roach LS, Ismagilov RF. A droplet-based, composite PDMS/glass capillary microfluidic system for evaluating protein crystallization conditions by microbatch and vapor-diffusion methods with on-chip X-ray diffraction. *Angew Chem Int Edit*. 2004;43:2508–2511.
30. Su YH, Chen GW, Zhao YC, Yuan Q. Intensification of liquid-liquid two-phase mass transfer by gas agitation in a microchannel. *AIChE J*. 2009;55:1948–1958.

31. Ahmed B, Barrow D, Wirtha T. Enhancement of reaction rates by segmented fluid flow in capillary scale reactors. *Adv Synth Catal*. 2006;348:1043–1048.
32. Chen WL, Twu MC, Pan C. Gas-liquid two-phase flow in microchannels. *Int J Multiphas Flow*. 2002;28:1235–1247.
33. Akbar MK, Plummer DA, Ghiaasiaan SM. On gas-liquid two-phase flow regimes in microchannels. *Int J Multiphas Flow*. 2003;29:855–865.
34. Yue J, Luo LG, Gonthier Y, Chen GW, Yuan Q. An experimental investigation of gas-liquid two-phase flow in single microchannel contactors. *Chem Eng Sci*. 2008;63:4189–4202.
35. Salman W, Gavriilidis A, Angeli P. Axial mass transfer in Taylor flow through circular microchannels. *AIChE J*. 2007;53:1413–1428.
36. Fournier MC, Falk L, Villermaux J. A new parallel competing reaction system for assessing micromixing efficiency - Determination of micromixing time by a simple mixing model. *Chem Eng Sci*. 1996;51:5187–5192.
37. Guichardon P, Falk L, Villermaux J. Extension of a chemical method for the study of micromixing process in viscous media. *Chem Eng Sci*. 1997;52:4649–4658.
38. Guichardon P, Falk L. Characterisation of micromixing efficiency by the iodide-iodate reaction system. Part I: experimental procedure. *Chem Eng Sci*. 2000;55:4233–4243.
39. Günther A, Jhunjhunwala M, Thalmann M, Schmidt MA, Jensen KF. Micromixing of miscible liquids in segmented gas-liquid flow. *Langmuir*. 2005;21:1547–1555.
40. Garstecki P, Fuerstman MJ, Stone HA, Whitesides GM. Formation of droplets and bubbles in a microfluidic T-junction-scaling and mechanism of break-up. *Lab Chip*. 2006;6:437–446.
41. Van Steijn V, Kreutzer MT, Kleijn CR. μ-PIV study of the formation of segmented flow in microfluidic T-junctions. *Chem Eng Sci*. 2007;62:7505–7514.
42. Günther A, Khan SA, Thalmann M, Trachsel F, Jensen KF. Transport and reaction in microscale segmented gas-liquid flow. *Lab Chip*. 2004;4:278–286.
43. Yue J, Luo LG, Gonthier Y, Chen GW, Yuan Q. An experimental study of air–water Taylor flow and mass transfer inside square microchannels. *Chem Eng Sci*. 2009;64:3697–3708.
44. Warnier MJF., Rebrov EV, de Croon MHJM, Hessel V, Schouten JC. Gas hold-up and liquid film thickness in Taylor flow in rectangular microchannels. *Chem Eng J*. 2008;135:S153–S158.
45. Yun JX, Lei Q, Zhang SH, Shen SH, Yao KJ. Slug flow characteristics of gas-miscible liquids in a rectangular microchannel with cross and T-shaped junctions. *Chem Eng Sci*. 2010;65:5256–5263.
46. Fries D, von Rohr PR. Impact of inlet design on mass transfer in gas-liquid rectangular microchannels. *Microfluid Nanofluid*. 2009;6:27–35.
47. Pohorecki R, Kula K. A simple mechanism of bubble and slug formation in Taylor flow in microchannels. *Chem Eng Res Des*. 2008;86:997–1001.
48. Liu H, Vandu CO, Krishna R. Hydrodynamics of Taylor flow in vertical capillaries: flow Regimes, bubble rise velocity, liquid slug length, and pressure drop. *Ind Eng Chem Res*. 2005;44:4884–4897.
49. Zheng B, Tice JD, Ismagilov RF. Formation of droplets and mixing in multiphase microfluidics at low Reynolds and capillary numbers. *Langmuir*. 2003;19:9127–9133.
50. Kreutzer MT, Kapteijn F, Moulijn JA, Heiszwolf JJ. Multiphase monolith reactors: chemical reaction engineering of segmented flow in microchannels. *Chem Eng Sci*. 2005;60:5895–5916.
51. Aussillous P, Quéré D. Quick deposition of a fluid on the wall of a tube. *Phys Fluids*. 2000;12:2367–2371.
52. Kreutzer MT, Du D, Heiszwolf JJ, Kapteijn F, Moulijn JA. Mass transfer characteristics of three-phase monolith reactors. *Chem Eng Sci*. 2001;56:6015–6023.
53. Vandu CO, Liu H, Krishna R. Mass transfer from Taylor bubbles rising in single capillaries. *Chem Eng Sci*. 2005;60:6430–6437.
54. Tanthapanichakoon W, Aoki N, Matsuyama K, Mae K. Design of mixing in microfluidic liquid slugs based on a newdimensionless number for precise reaction and mixing operations. *Chem Eng Sci*. 2006;61:4220–4232.

Manuscript received Jan. 3, 2011, and revision received May 19, 2011.